Food Science and Biotechnology (2024) 33:2189–2200
https://doi.org/10.1007/s10068-024-01530-2

RESEARCH ARTICLE

Probiotic and immunostimulating effects of live and heat-killed *Pediococcus pentosaceus* TAP041

Chaeeun Lee[1] · Young-Seo Park[1]

Received: 16 November 2023 / Revised: 10 January 2024 / Accepted: 15 January 2024 / Published online: 19 February 2024

Abstract
The selected strain, TAP041, showing an excellent ability to reduce the glyoxal and methylglyoxal levels, was identified by 16S rRNA gene-based phylogenetic analysis as *Pediococcus pentosaceus*. It demonstrated probiotic properties, including acid, bile salt, pancreatin, lysozyme tolerance, gut adhesion, and auto/coaggregation. In RAW264.7 macrophages, both live and heat-killed strains induced nitric oxide production and activated inducible nitric oxide synthase. RAW264.7 treated with *P. pentosaceus* TAP041 increased the expression level of tumor necrosis factor-α, interleukin (IL)-1β, IL-6, and cyclooxygenase-2, and regulated the expression of c-Jun amino-terminal kinase, p38, and extracellular signal-regulated kinase. These findings suggest that both live and heat-killed *P. pentosaceus* TAP041 can be used as potential immunostimulatory agents in functional food additives.

Keywords Probiotics · Immunostimulating activity · *Pediococcus pentosaceus* · Heat-killed probiotics

Introduction

According to the Food and Agriculture Organization/World Health Organization (FAO/WHO, 2002), probiotics are defined as "live microorganisms that, when administered in adequate amounts, confer a health benefit on the host." The guidelines presented by the FAO/WHO (2002) for in vitro testing of probiotic strains include: resistance to gastric acidity, bile acid resistance, adherence to mucus and/or human epithelial cells and cell lines, antimicrobial activity against potentially pathogenic bacteria, and the ability to reduce pathogen adhesion to surfaces. To function as probiotics in the human gastrointestinal tract, strains must survive extreme conditions, such as low acid, bile salt, and digestive enzymes (Cao et al., 2015; Cho et al., 2023; Pramanik et al., 2023).

Some strains of *Lactobacillus* and *Bifidobacterium* are known as probiotics (García-Ruiz et al., 2014). *P. pentosaceus* belongs to the family *Lactobacillaceae* and the genus *Pediococcus*, and is a homofermentative lactic acid bacterium (LAB) that is facultatively anaerobic, Gram-positive, and cocci-shaped. Many studies have confirmed that *P. pentosaceus* has potential probiotic effects, including cholesterol-lowering capacity, immune system enhancement, and prevention of cardiovascular diseases (Kwon et al., 2018; Shin et al., 2016; Zhang et al., 2022).

Glyoxal (GO) and methylglyoxal (MGO), reactive α-dicarbonyl compounds, are commonly found in food and are precursors of advanced glycation end products (AGEs). They are produced primarily during the Maillard reaction, lipid oxidation, and sugar degradation (Gaens et al., 2013). MGO accumulation has been shown to induce oxidative stress in rats and MC3T3-E1 cells, and continuous accumulation may lead to neurological disorders, such as Alzheimer's and Parkinson's disease (Sena et al., 2012; Suh et al., 2014). Since GO and MGO are first encountered in the human gut, inhibition of their activity should occur primarily in the gut. The accumulation of glycated proteins strongly correlates with the progression of neurodegenerative diseases and diabetes complications; thus, developing a dietary agent aimed at attenuating glycated proteins is important (Lin et al., 2023).

This study aimed to isolate LAB with the ability to reduce the levels of GO and MGO, validate the probiotic attributes

✉ Young-Seo Park
ypark@gachon.ac.kr

Chaeeun Lee
dlcodms1212@gmail.com

[1] Department of Food Science and Biotechnology, Gachon University, Seongnam 13120, Republic of Korea

of the selected strain, and investigate their potential impacts on immune-related responses.

Materials and methods

Bacterial strains and culture media

To isolate the MGO-tolerant strains, 987 strains stored at the Korean Culture Collection of Probiotics (KCCP; Seongnam, Korea) were screened. *Lactococcus lactis* KF140 (KCCM 11673 1028P) was provided by the Korean Culture Center of Microorganisms (KCCM; Seoul, Korea). *Lactobacillus rhamnosus* GG ATCC 53103 was obtained from the American Type Culture Collection (ATCC; Manassas, VA, USA). All LAB strains were cultured in de Man, Rogosa, and Sharpe broth (MRS; BD, Franklin Lakes, NJ, USA).

The pathogenic bacteria *Salmonella* Typhimurium ATCC 14028 and *Escherichia coli* ATCC 10536 were provided by ATCC, while *Bacillus cereus* KCCM 11204, *Listeria monocytogenes* KCCM 40307, *Staphylococcus aureus* subsp. *aureus* KCCM 40881, and *Klebsiella pneumoniae* subsp. *pneumoniae* KCCM 41433 were obtained from KCCM. *B. cereus, S.* Typhimurium, *S. aureus* subsp. *aureus*, and *K. pneumoniae* subsp. *pneumoniae* were cultured in nutrient broth (BD Biosciences), *E. coli* was cultured in tryptic soybean broth (BD Biosciences), and *L. monocytogenes* were cultured in brain heart infusion broth (BD Biosciences).

Screening of methylglyoxal-resistant lactic acid bacteria

The 987 LAB strains were cultured in 1 mL MRS broth at 37 ℃ for 20 h (seed culture) followed by inoculation at a concentration of 1% (v/v) into MRS broth added with 5 mM MGO (Sigma-Aldrich, St. Louis, MO, USA). To monitor the growth of the LAB strain selected from the screening, the seed culture was inoculated at a concentration of 2% into MRS broth containing four different concentrations of MGO (0, 0.5, 1.0, and 2.0 mM). Subsequently, these cultures were incubated at 37 ℃ for 7 h. Cell growth was measured every hour at an absorbance wavelength of 600 nm using an Epoch microplate reader (BioTek Instruments Inc., Winooski, VT, USA).

Quantitative measurement of glyoxal and methylglyoxal by high-performance liquid chromatography

The quantitative evaluation of GO and MGO was performed using a modified method of Uğur et al. (2022). The LAB seed culture was inoculated at 1% (v/v) into MRS broth supplement with 200 µg/mL GO and 720 µg/mL MGO, respectively, followed by incubation at 37 ℃ for 48 h. The culture was centrifuged at 14,000 g for 5 min, and the initial incubation time (0 h) served as a control. The supernatant (0.5 mL) was taken into a 5 mL screw tube, to which 1 mL of sodium acetate buffer (0.1 M; pH 3.6) and 0.5 mL of derivatization solution (4-nitro-1,2-phenylenediamine in 1% methanol) were sequentially added. The mixture was incubated at 70 ℃ for 20 min and was filtered through a 0.22 µm polyvinylidene fluoride filter (SMARTiLAB, Seoul, Korea).

High-performance liquid chromatography (HPLC) analysis was performed using a DIONEX UltiMate 3000 HPLC system (Thermo Fisher Scientific Inc., Waltham, MA, USA). A C-18 column (Model number: TC-C18(2), 250 × 4.6 mm, ID 5 µm; Agilent Technologies, Inc., Santa Clara, CA, USA) was used while detection occurred via an ultraviolet detector to wavelength of 255 nm. The column oven temperature was maintained at 30 ℃ while the sample injection volume used was 20 µL. The mobile phase was a methanol:water:acetonitrile mixture with a ratio of 42:56:2 (v/v/v), and the samples were eluted isocratically at a flow rate of 1 mL/min.

Identification of lactic acid bacteria

16S rRNA gene sequencing and phylogenetic tree

The selected strain was cultured in MRS broth, and genomic DNA was extracted using the AccuPrep Genomic DNA Extraction Kit (Bioneer, Seoul, Korea). The 16S rRNA sequence was amplified using the universal primers 27F and 1492R in a TurboCycler 2 Thermal Cycler (BLUERAY Biotech, New Taipei City, Taiwan). The polymerase chain reaction (PCR) conditions involved pre-denaturation at 94 ℃ for 2 min and 35 cycles of denaturation at 94 ℃ for 30 s, annealing at 50 ℃ for 1 min, and extension at 72 ℃ for 1 min. The post-extension step was conducted at 72 ℃ for 7 min. Phylogenetic analyses were performed as described by Lee et al. (2022).

Scanning electron microscopy

The cellular morphology of the strain was examined using a H-7600 scanning electron microscope (SEM; Hitachi, Tokyo, Japan) located at Eulji University (Seongnam, Korea). This process was performed as described by Lee et al. (2022).

The carbohydrates fermentation profiling of lactic acid bacteria

The colonies were suspended to reach a concentration of 0.5 McFarland (0.05 mL of 1.175% barium chloride dihydrate with 9.95 mL of 1% sulfuric acid) (cell density at

1.5×10^8 CFU/mL). This suspension was inoculated into API 50 CHL medium (BioMérieux, I' Etole, France) and dropped onto API 50 CH strips. These strips were incubated at 37℃ for 48 h, and carbohydrate utilization was interpreted using APIweb (http://apiweb.biomerieux.com).

Tolerance of selected strain to acid, bile salt, pancreatin, and lysozyme

To determine acid tolerance, the seed culture of the strain was inoculated into MRS broth at a 1% (v/v) concentration and allowed to grow at 37 ℃ for 16 h. The culture was centrifuged at 16,000 × g for 1 min and then washed thrice with 0.88% (w/v) NaCl. The pellets were resuspended in 4 mL glycine–HCl buffer (0.1 M, pH 2.5), with this cell resuspension incubated at 37 ℃ for 2 h without stirring. One hundred microliters of decimal dilutions were spread onto an MRS agar plate and incubated at 37 ℃ for 20 h. Viable cells were quantified as colony-forming units per mL (CFU/mL). Acid tolerance was calculated using the following equation:

$$\text{Acid tolerance}(\%) = \frac{\text{Viable cell number after 2h reaction}(\log\text{CFU/mL})}{\text{Initial viable cell number}(\log\text{CFU/mL})} \times 100$$

To determine bile salt and pancreatin tolerance, the seed culture was inoculated at a concentration of 1% (v/v) to MRS supplemented with 0.3% (w/v) oxgall (BD) or 0.5% (w/v) pancreatin (Sigma-Aldrich), respectively, and followed by incubation at 37 ℃ for 24 h. Viable cell counts were determined similarly to the acid tolerance test, and bile salt or pancreatin tolerance was calculated as follows:

$$\text{Bile salt or pancreatin tolerance}(\%) = \frac{\text{Viable cell number after 24h reaction}(\log\text{CFU/mL})}{\text{Initial viable cell number}(\log\text{CFU/mL})} \times 100$$

The lysozyme tolerance of the strain was examined using a modified method of Tarique et al. (2022). The seed culture of the strain was inoculated into lysozyme solution (0.22 g $CaCl_2$, 6.2 g NaCl, 2.2 g KCl, 1.2 g $NaHCO_3$, and 0.1 g lysozyme (Sigma-Aldrich), per liter) to achieve a concentration of 10% (v/v). After incubation of the bacterial suspensions at 37 °C for 90 min, decimal dilutions of the bacterial suspensions were performed as described above. Lysozyme tolerance was calculated using the following equation:

$$\text{Lysozyme tolerance}(\%) = \frac{\text{Viable cell number after 90min reaction}(\log\text{CFU/mL})}{\text{Initial viable cell number}(\log\text{CFU/mL})} \times 100$$

Adherent ability to Caco-2 cells

Caco-2 cells were grown at a density of 5×10^5 cells/well and cultured until 80–90% covered surface areas at 37 °C with 5% CO_2. Caco-2 cells were then exposed to bacterial cells at a multiplicity of infection (MOI; the ratio of the number of LAB to the number of macrophage cells) of 1000 (5×10^8 CFU) in each well, followed by incubation at 37 °C for 2 h. Post-incubation, any non-adherent bacteria on the cell surface were rinsed off twice using Dulbecco's phosphate buffered saline (DPBS; Welgene Inc., Gyeongsan, Korea) and detached from plates using a solution of 0.25% trypsin–EDTA. To release the adherent bacterial cells, 0.1% (v/v) Triton X-100 diluted in DPBS was added to the cells. Finally, the suspension was spread onto MRS agar plate, which was subsequently incubated at 37 °C for 20 h. A sample without Caco-2 cells in a microcentrifuge tube served as a control. The adhesion ability was determined as the percentage ratio between viable cell numbers in the sample (log CFU/mL) and those in the control (log CFU/mL).

Auto-/coaggregation

The auto- and coaggregation capacities of the strains were measured using the method described by Ohn et al. (2020). Pellets of cultured LAB and pathogenic bacteria were washed twice with phosphate-buffered saline (PBS), and the optical density (OD_{600}) was adjusted to 0.3 at PBS in a cuvette. The OD_{600} was measured at 0, 2, 5, 10, 24, 36, and 48 h at 37 °C using a spectrophotometer (BioSpec-mini; Shimadzu Co., Kyoto, Japan).

The coaggregation assay was performed using the same method described for the auto-aggregation assay. The OD_{600} of a mixture of LAB and pathogenic bacteria at a ratio of 1:1 was measured at 0, 2, 5, 8, 12, 24, 36, and 48 h at 37 ℃. Auto-/co-aggregation was calculated as described by Tarique et al. (2022):

$$\text{Auto} - \text{aggregation, Coaggregation}(\%) = \left[1 - \frac{A_{\text{time}}}{A_{\text{initial}}}\right] \times 100$$

where "A_{time}" is the absorbance at the different incubation times and "$A_{initial}$" is the absorbance at the initial time.

Immunostimulating activity

Cell culture and lactic acid bacteria preparation

RAW264.7 macrophage cells were cultured in Dulbecco's modified Eagle's medium (DMEM; Gibco, Grand Island, NY, USA) supplemented with 10% fetal bovine serum (Gibco) and 1% penicillin–streptomycin (Gibco) and incubated at 37 ℃ with 5% CO_2 atmosphere. The seed culture of LAB was inoculated into MRS broth at a concentration of 1% (v/v) and cultivated at 37 °C until it reached a density

of 5×10^8 CFU/mL. This culture was then centrifuged at 16,000 × g, 4 ℃ for 1 min, and the collected cells were rinsed twice with DPBS to prepare the live LAB sample. These harvested cells were heat-killed at 121 °C for 15 min to prepare the heat-killed LAB sample used in subsequent experiments.

Cell viability

The RAW264.7 macrophages were seeded into a 96-well plate at a density of 5×10^4 cells/well and incubated at 37 ℃ for 20 h. These cells were exposed to both live and heat-killed *P. pentosaceus* TAP041 at MOI 62.5–1000. Following a 24 h incubation at 37 ℃, the supernatant was removed, and the plate was washed twice with DPBS. The plate was incubated to DMEM along with the addition of EZ-cytox (DoGenBio Co., Ltd., Seoul, Korea) for 40 min. The absorbance of each well was measured at 450 nm using a microplate reader, and cell viability was calculated.

Nitric oxide assay

RAW264.7 cells were seeded into a 24-well plate at a density of 5×10^5 cells/well and incubated at 37 ℃ for 20 h. The RAW264.7 cells were treated with live and heat-killed LAB and 1 μg/mL of lipopolysaccharides (LPS; Sigma-Aldrich) as a positive control. After incubation for 24 h, NO levels were determined using the Griess reagent. The supernatants were collected into a new tube, and 100 μL supernatant was transferred to a 96-well plate. Griess reagents A (0.1% *N*-(1-naphthyl) ethylenediamine dihydrochloride in water) and B (1% sulphanilamide in 2.5% phosphoric acid) were added to be equivalent to supernatants. The produced nitric oxide was detected at 540 nm using a microplate reader, and the 0–250 μM sodium nitrite (Samchun chemicals, Seoul, Korea) was used to generate a standard curve.

Real-time quantitative polymerase chain reaction

The mRNA expression level of inducible NO synthase (iNOS), tumor necrosis factor-α (TNF-α), interleukin (IL)-6, IL-1β, and cyclooxygenase (COX)-2 on the cells was evaluated by real-time quantitative PCR (RT-qPCR). The seeded RAW264.7 cells in a 6-well plate at 1×10^6 cells/well cultured for 20 h, and live LAB (MOI 250), heat-killed LAB (MOI 500), and LPS (1 μg/mL) were treated each for 24 h. After washing the cells twice with DPBS, total RNA was isolated using an Easy-BLUE Total RNA extraction kit (iNtRON Biotechnology Inc., Seongnam, Korea). The isolated total RNA was quantified by nanodrop (Epoch microplate reader, BioTek Instruments Inc.), and 1 μg RNA was used to prepare cDNA. Template DNA was prepared using CellScript™ cDNA master mix (CellSafe, Suwon, Korea), and RT-qPCR analysis was performed with QuatStudio™ 1 Real-Time PCR system (Thermo Fisher Scientific Inc.) using the QgreenBlue™ 2X PCR master mix (CellSafe) according to the manufacturer's instructions. The detailed primer sequences are listed in Table S1.

Western blot

Sample-treated RAW264.7 cells were prepared for RT-qPCR as described above. After washing the cells twice with DPBS, cell lysis was performed using PRO-PREP Protein extraction solution (iNtRON Biotechnology). Protein contents in the lysate were quantified using the Pierce™ BCA protein assay kit (Thermo Fisher Scientific Inc.). Each sample containing 50 μg of protein was loaded onto a 9% SDS-PAGE and transferred onto a nitrocellulose membrane. This membrane was blocked for 30 min at 25 ℃ with a solution of 3% (w/v) bovine serum albumin fraction V (Roche, Basel, Switzerland) in Tris-buffered saline with Tween-20 (TBST, iNtRON Biotechnology). The membrane was then exposed to rabbit primary antibodies targeting p-c-Jun amino-terminal kinase (JNK), JNK, p-extracellular signal-regulated kinase (ERK), p-p38, p38, and β-actin (Cell Signaling Technology Inc., Danvers, MA, USA) at 25 ℃ for 1 h and washed with TBST for 45 min. The membrane was incubated with anti-rabbit IgG-HRP-conjugated secondary antibody (Cell Signaling Technology) at 25 ℃ for 1 h and washed four times with TBST. EzWestLumi Plus (ATTO Corporation, Tokyo, Japan) was used as the chemiluminescent substrate. The protein bands were visualized using Amersham™ Imager 600 (GE Healthcare, Chicago, IL, USA) and quantified using Image J software (National Institutes of Health, Bethesda, MD, USA). The protein expression levels were determined by comparison to β-actin.

Statistical analysis

All results are expressed as mean ± standard deviation for experiments performed in triplicate. Statistical analyses were performed using IBM SPSS Statistics version 28.0 (SPSS Inc. Chicago, IL, USA). Statistical significance was estimated using a one-way analysis of variance (ANOVA) with

Duncan's multiple-range test. Statistical significance was set at p values < 0.05.

Results and discussion

Strain selection and GO and MGO degradation

The growth of the 987 LAB strains was assessed in MRS broth supplemented with 5 mM MGO, and the strain TAP041 with the highest MGO reduction ability was selected (data not shown). *L. lactis* KF140 exhibited an ability to reduce the level of N^{ε}-(carboxymethyl)lysine (CML), a type of AGE derived from GO, and served as a positive control (Park et al., 2022). When the growth of strain TAP041 and *L. lactis* KF140 was monitored in co-incubation with varying concentrations of MGO from 0 to 2.0 mM, both strains exhibited the highest growth rates in MRS broth without MGO for 7 h (Fig. S1). However, adding MGO to the broth resulted in dose-dependent growth inhibition. At a concentration of 2 mM MGO, the growth of *L. lactis* KF140 was inhibited more than that of strain TAP041.

As shown in Fig. S2, the initial GO level at 95.2 ppm was reduced by co-incubation with *L. lactis* KF140 and strain TAP041 by 25.4% and 31.4%, respectively. Similarly, the initial MGO level at 523 ppm decreased to 8.4% when co-incubated with *L. lactis* KF140 and to 5.6% when co-incubated with strain TAP041. Compared to *L. lactis* KF140, strain TAP041 demonstrated higher efficacy in reducing MGO levels. However, these results alone do not conclusively establish *the* in vivo AGE-reducing activity of strain TAP041; thus, further investigation is required to elucidate the anti-glycation mechanism of this strain.

Identification of strains

As shown in Fig. 1, a phylogenetic analysis was performed using the nucleotide sequence of the 16S rRNA gene of strain TAP041. The morphology of strain TAP041 is characterized by the diameter of 1.0–1.2 µm forming tetrads, a characteristic feature of *Pediococcus* spp. The genus *Pediococcus* is spherical, 1.0–2.0 µm in diameter, and tetrads form (Holt et al., 1994). When the carbohydrate utilization of strain TAP041 was compared with that of the type strain *P. pentosaceus* KCCM 11902, it was observed that strain TAP041 could utilize D-melibiose, D-saccharose, D-raffinose, and potassium gluconate, not used by type strain KCCM 11902, which was similar to the type strain *P. pentosaceus* KCCM 11902 (Table S3). Based on these results, strain TAP041 was identified as *P. pentosaceus*.

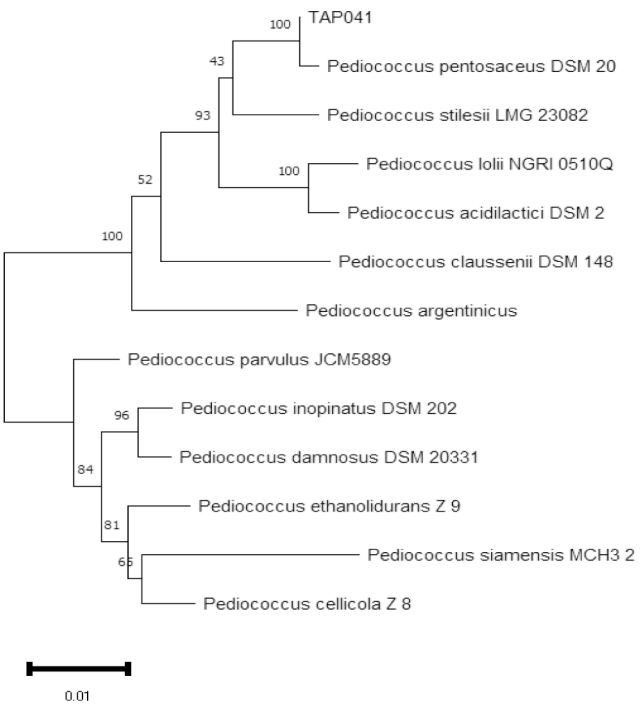

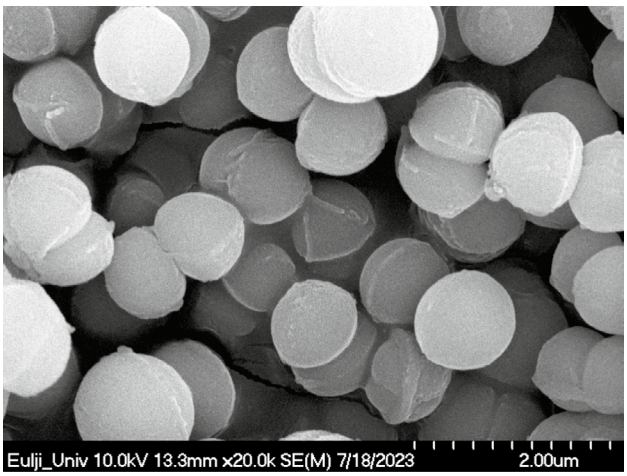

Fig. 1 Phylogenetic tree of *P. pentosaceus* TAP041 based on the sequence of the 16S rRNA gene and the scanning electron microscopy images of *P. pentosaceus* TAP041. (Left panel) Neighbor-joining method was used to construct the phylogenetic tree, using 16S rRNA sequences for analysis. (Right panel) Scanning electron microscopy (×20,000)

In vitro resistance to acid, bile salt, pancreatin, and lysozyme

When the *P. pentosaceus* TAP041 and LGG were exposed to acid, bile salts, pancreatin, and lysozyme, their tolerance to acidic environments (pH 2.5) of *P. pentosaceus* TAP041 was 63.4%, and that of LGG was 64.9% (Table 1). Survival at low-pH conditions is an important factor in selecting potential probiotics to ensure their viability and functionality. *P. pentosaceus* TAP041 and LGG exhibited 82.9% and 88.8% bile tolerances, respectively. Bile salts generally act as detergents that damage the lipid membranes of bacterial cells (Abdalla et al., 2021). The resistance of a strain to bile salts is related to the enzymatic activity of the bile salt hydrolase, which is involved in the hydrolysis of conjugated bile, thereby alleviating toxicity (du Toit et al., 1998). The survival rate of *P. pentosaceus* TAP041 did not decrease in pancreatin and lysozyme tolerance tests. Pancreatic enzymes are secreted into the small intestine and are involved in food digestion. Lysozymes present in the saliva have antimicrobial activity. In acid, bile salt, and lysozyme tolerance tests, the viable cell count of *P. pentosaceus* TAP041 was higher than that of *P. pentosaceus* CRAG3 (Shukla and Goyal, 2014). In general, probiotics are considered more effective if there is a minimal reduction in viable bacterial counts in an in vitro tolerance test (Ayyash et al., 2021). The four tolerance tests of *P. pentosaceus* TAP041 were similar to those of a well-known probiotic strain, LGG, suggesting the potential of *P. pentosaceus* TAP041 as a probiotic strain.

Gut-adhesion ability

P. pentosaceus TAP041 and LGG confirmed the same levels of adhesion rate of 88.4% (Table 1). LGG is a representative probiotic strain recognized for its high adhesion to gastrointestinal cells, and its ability to adhere to the mucosal membranes of the gastrointestinal tract is a pivotal characteristic of probiotic strains. *Leuconostoc lactis* CCK940, *L. lactis* SBC001, and *Weissella cibaria* YRK005 show different adhesion rates (54.2–67.6%) (Jeong et al., 2023). *P. acidilactici* MTCC5101 showed strong adhesion to the villi of Caco-2 cells (150%) and was observed to adhere to each other (Balgir et al., 2013). Thus, the intestinal adherence of *P. pentosaceus* TAP041 was similar to that of LGG and could be used as a probiotic strain.

Auto/coaggregation ability

As shown in Fig. 2A, the auto-aggregation ability of *P. pentosaceus* TAP041 at 48 h was 66.6%, comparable to that observed in LGG (71.2%). Whereas, pathogenic strains generally showed a higher ability to auto-aggregation, at the level of 82.2% for *L. monocytogenes* and that of 91.1 ± 0.8% for *B. cereus*. Auto-aggregation of some *P. pentosaceus* strains (65.2–69.1%) was exhibited higher than that of *P. pentosaceus* TAP041 (53.0%) at 24 h (Lee et al., 2014). It is reported that aggregation ability increases in a time-dependent manner (Joung et al., 2023). It has also been reported that strains with a strong ability to auto-aggregate have high adhesion to the intestinal tract (Ocaña and Nader-Macías, 2002). Different autoaggregation levels between strains may be due to factors such as bacterial cell surface structure and adhesion mechanisms. Autoaggregation has been frequently observed in pathogenic bacteria and can increase their tolerance to antimicrobial activity. In the aggregated state of probiotics, pathogens are neutralized and unable to colonize the mucosal surface of the host (Trunk et al., 2018).

When coaggregation of *P. pediococcus* TAP041 and LGG with some pathogens was examined, *P. pentosaceus* TAP041 showed the best coaggregation rate with *B. cereus* (76.7 ± 0.4%) (Fig. 2B-C). For LGG, the best result was observed with *B. cereus* (78.1 ± 8.7%). *B. cereus* exhibits a robust survival capacity in the intestinal tract, which is attributed to factors such as biofilm formation (Lin et al., 2022). *P. pentosaceus* TAP041 and LGG had 74.3 ± 1.4% and 69.2 ± 1.2% coaggregation with *E. coli*, respectively. Strains with high auto-aggregation ability were also found to have high coaggregation ability. The two LAB strains showed coaggregation abilities with pathogenic bacteria, and the degree of coaggregation varied depending on the species or strain (Lee et al., 2014).

Immunostimulating activity

As shown in Fig. 3A, RAW264.7 cells treated with *K. pneumoniae* subsp. *pneumoniae* exhibited 52.8% of cell

Table 1 Acid, bile salt, pancreatin, and lysozyme tolerance and gut adhesion ability of *P. pentosaceus* TAP041 and *L. rhamnosus* GG

Strain	Survival rate (%)				
	Acid tolerance	Bile tolerance	Pancreatin tolerance	Lysozyme tolerance	Gut adhesion ability
P. pentosaceus TAP041	63.4 ± 2.0	82.9 ± 1.1	98.5 ± 1.0	99.2 ± 0.6	88.4 ± 1.6
L. rhamnosus GG	64.9 ± 3.9	88.8 ± 0.9	100.3 ± 2.4	100.6 ± 1.0	88.4 ± 1.2

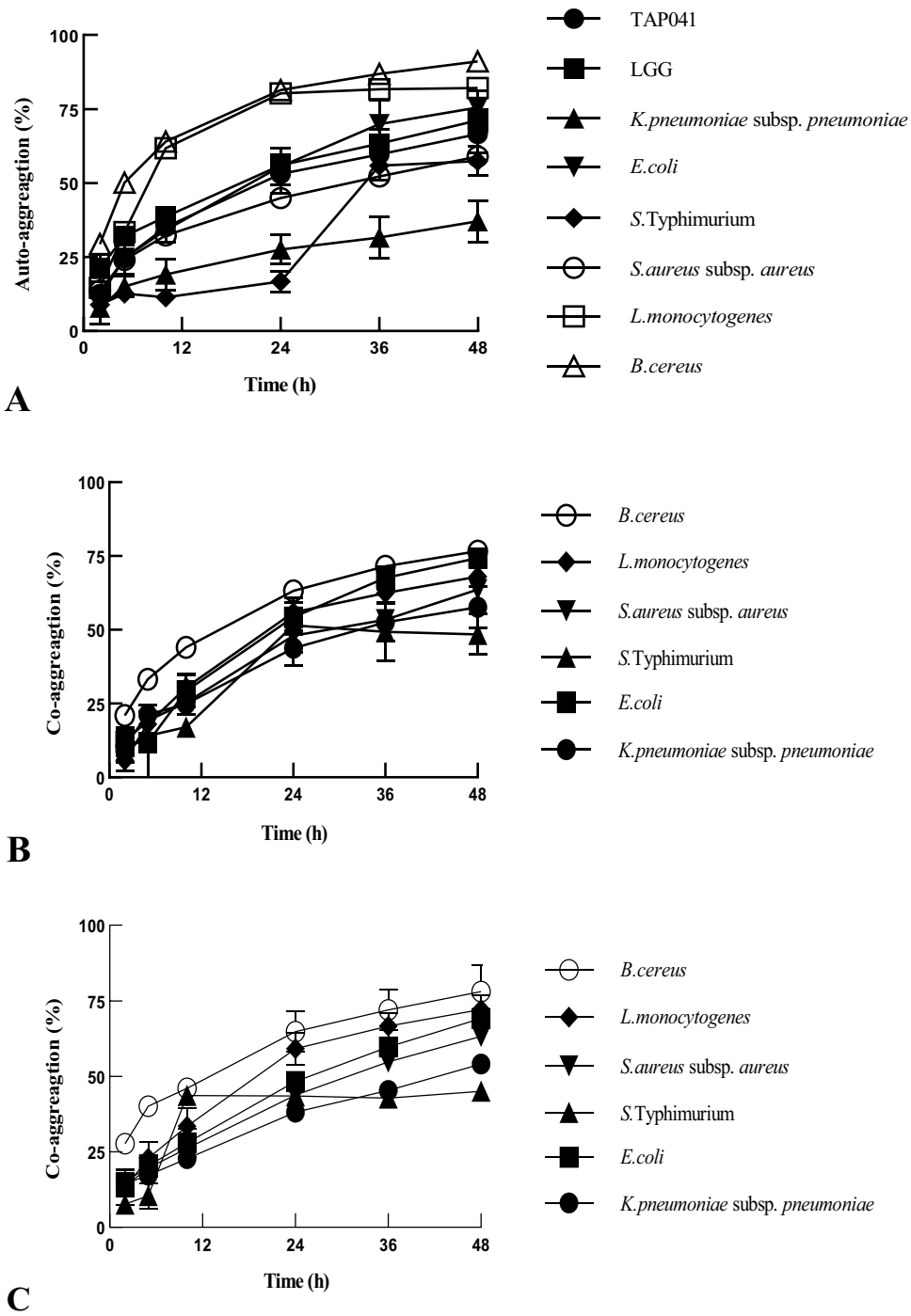

Fig. 2 Auto/Coaggregation of lactic acid and pathogenic bacteria over incubation time at 37 ℃. The pellets of *P. pentosaceus* TAP041, LGG, and six pathogenic bacterial strains were suspended in PBS, and the optical density (OD_{600}) was adjusted to 0.3 in a cuvette. OD_{600} was measured at 0, 2, 5, 10, 24, 36, and 48 h. **A** auto-aggregation of lactic acid bacteria and pathogens, **B** coaggregation of *P. pentosaceus* TAP041 against pathogens, **C** coaggregation of LGG against pathogens. TAP041, *P. pentosaceus* TAP041; LGG, *Lactobacillus* GG

viability. The viability of RAW264.7 cells decreased as the cell numbers of live *P. pentosaceus* increased, and no cytotoxicity on RAW264.7 cells was observed up to MOI 500. Heat-killed bacteria showed no cytotoxicity up to an MOI of 1000. It was confirmed that the heat-killed LAB treatment was less toxic than the live cell treatment.

NO production in the live or heat-killed strains increased in an MOI-dependent manner (Fig. 3B–C). In the live *P. pentosaceus* TAP041-treated RAW264.7 cells (Fig. 3B), it was confirmed that the maximum production of NO produced by the macrophage cells treated with live *P. pentosaceus* TAP041 was 26.5 μM at MOI 62.5. At an MOI of 500, macrophages highly susceptible to NO-induced apoptosis may be affected by NO production (Coleman, 2001). Meanwhile, the production of NO in cells treated with heat-killed bacteria showed a significant increase of 19.1 ± 1.8 μM at

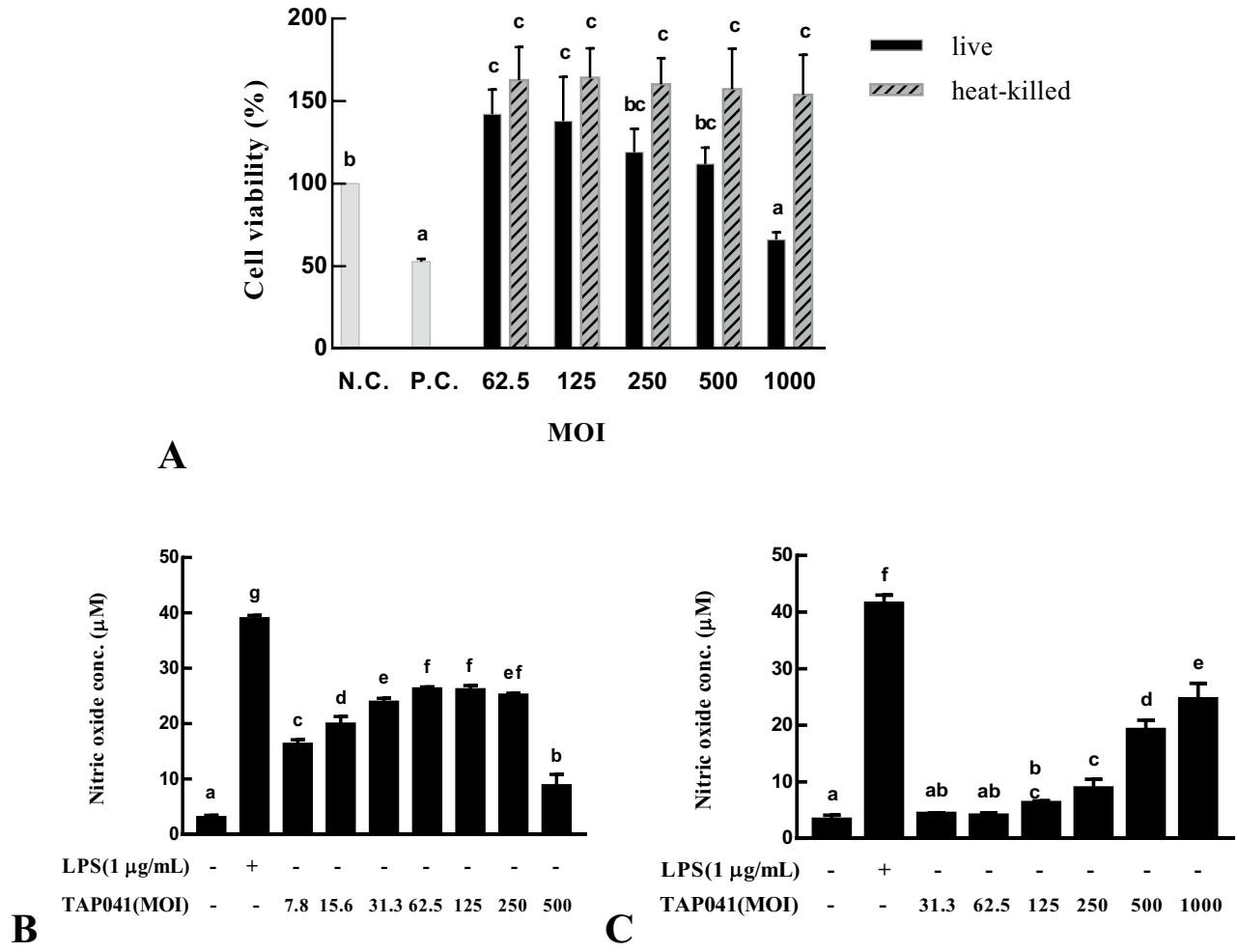

Fig. 3 Cytotoxicity and nitric oxide production of live and heat-killed *P. pentosaceus* TAP041 on RAW264.7 macrophages. **A** Viability of RAW264.7 cells. RAW264.7 cells were treated with live or heat-killed *P. pentosaceus* TAP041 at the concentrations (MOI 62.5–1000) or *K. pneumoniae* subsp. *pneumoniae* as a positive control for 24 h. **B** NO production was measured by Griess reagent in RAW264.7 cells treated with live *P. pentosaceus* TAP041. **C** NO production was measured by Griess reagent in RAW264.7 cells treated with heat-killed *P. pentosaceus* TAP041. N.C., negative control; P.C., *K. pneumonia* subsp. *pneumoniae* KCCM41433. Data represent the mean ± SD of three independent experiments

MOI 500 (Fig. 3C). Although excessive NO production is known to cause tissue damage due to an inflammatory response, an appropriate amount of NO can control microorganisms and cancer cells that cause intracellular infections (MacMicking et al., 1997). Thus, the increase in NO secretion following treatment with live or heat-killed *P. pentosaceus* TAP041 shows that *P. pentosaceus* TAP041 may stimulate immune activity, especially in heat-killed bacteria. NO, an indicator of macrophage activation, is a reactive nitrogen species produced by macrophages and is a gas molecule produced from L-arginine by NOS. The production of iNOS by LAB-treated macrophages with LAB showed similar to that of NO (Fig. 4A). It has been suggested that *P. pentosaceus* TAP041 regulates NO production in macrophages via NO- and iNOS-related signaling pathways and is involved in immune stimulation.

Among various cytokines, TNF-α and IL-6 are pro-inflammatory cytokines produced by activated immune cells during inflammation, and these cytokines can influence each other's secretion levels. As shown in Fig. 4B-C, when the gene expression levels of TNF-α and IL-6 in the untreated RAW264.7 cells were used as a negative control, and the cells treated with 1 μg/mL LPS showed a 16.8- and 259.5-fold increase, respectively. When RAW264.7 macrophages were treated with live LAB, the expression levels of TNF-α

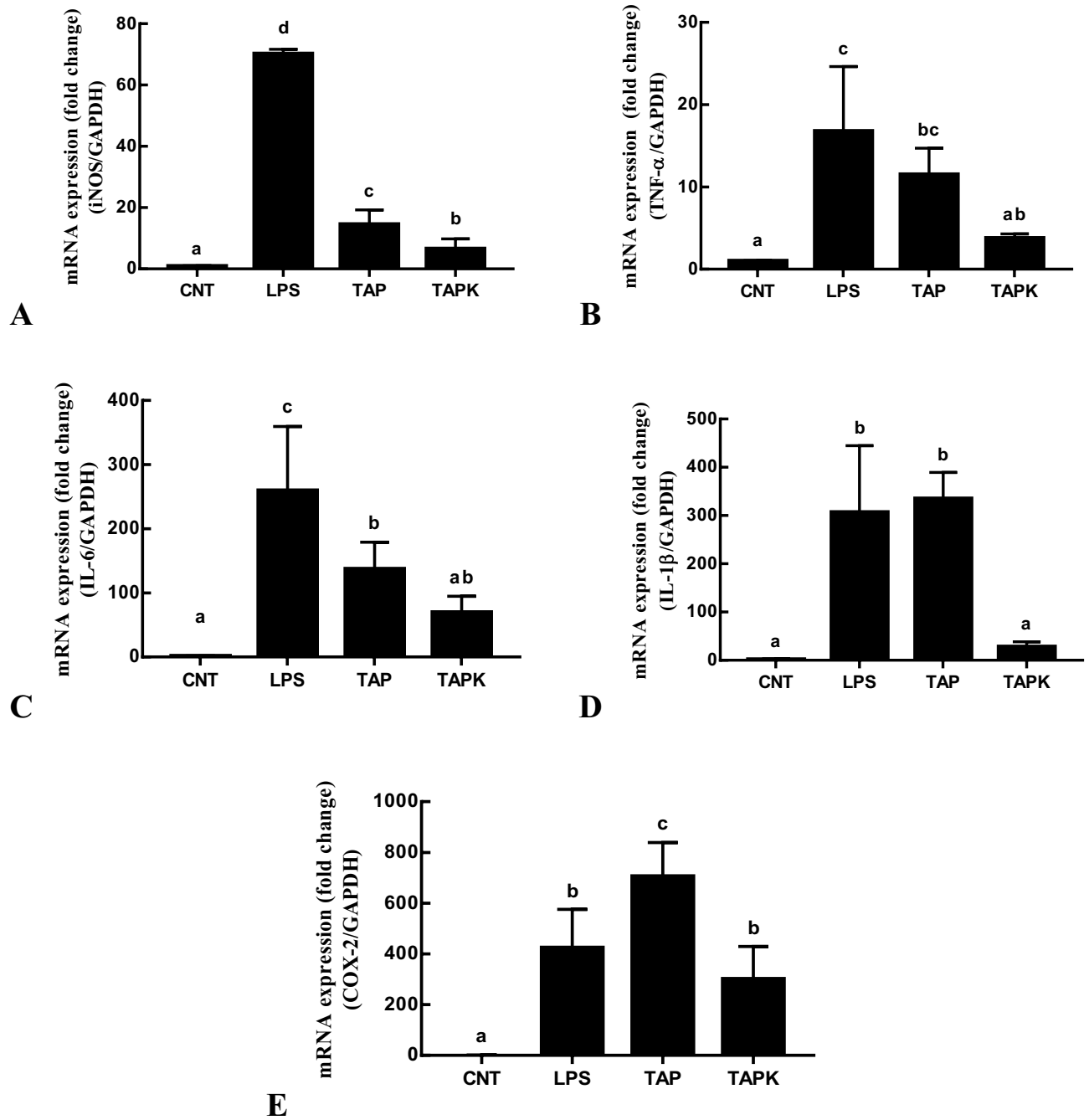

Fig. 4 The mRNA expression level of iNOS, TNF-α, IL-6, IL-1β, and COX-2-related immunostimulating activity of *P. pentosaceus* TAP041 in RAW 264.7 macrophages. The levels of **A** iNOS, **B** TNF-α, **C** IL-6, **D** IL-1β, and **E** COX-2 mRNA expression were determined by real-time qPCR, and the relative expressions of these genes were normalized to GAPDH. CNT, negative control; LPS, LPS-treated positive control; TAP, treated with live *P. pentosaceus* TAP041 (MOI 250); TAPK, treated with heat-killed *P. pentosaceus* TAP041 (MOI 500). Data depict the mean ± SD of three independent experiments

and IL-6 were 11.5- and 137.2-fold higher than those of heat-killed LAB (3.8- and 69.4-fold). The productions of TNF-α and IL-6 in macrophages treated with live and heat-killed LAB tended to increase in a similar way.

IL-1β and cyclooxygenase-2 (COX-2) expressions were also shown in Fig. 4D-E, and the expressions of IL-1β and COX-2 in LPS-treated macrophages were 306.5 and 423.4 fold, respectively, compared to non-treated cells. RAW264.7

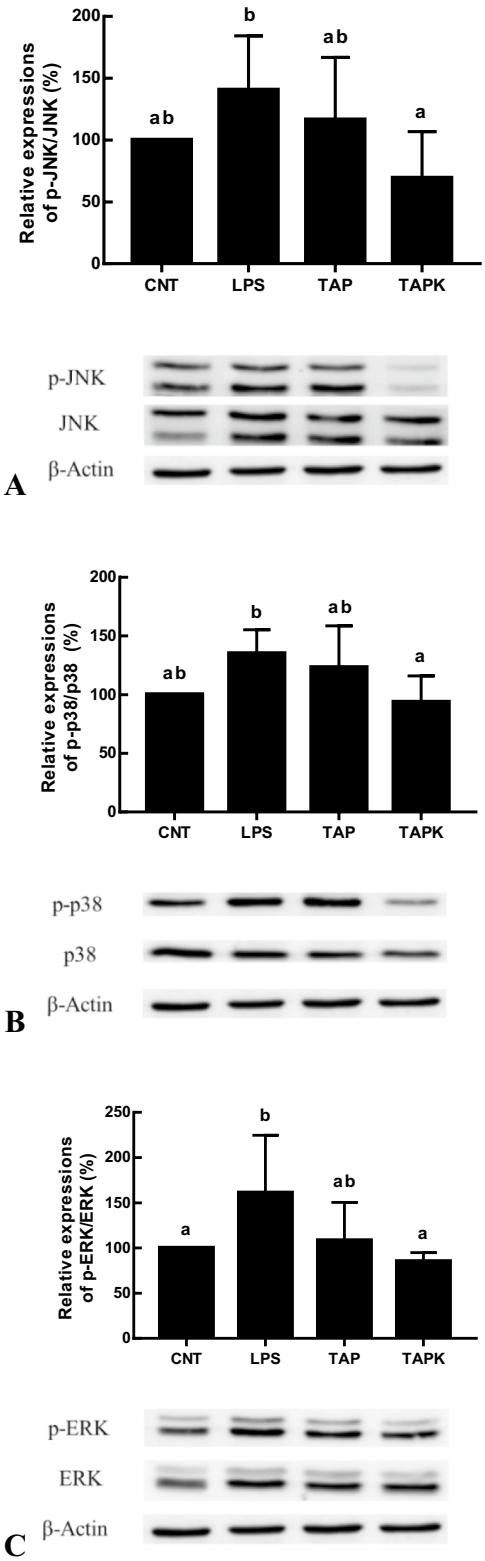

Fig. 5 Western blot analysis and relative protein levels of JNK, p38, and ERK. RAW 264.7 cells were co-cultured with *P. pentosaceus* TAP041 for 24 h. The relative protein expressions of **A** JNK, **B** p38, and **C** ERK of the MAPK pathway were measured by western blot analysis. CNT, negative control; LPS, LPS-treated positive control; TAP, RAW 264.7 cells were treated with live *P. pentosaceus* TAP041 (MOI250); TAPK, RAW 264.7 cells were treated with heat-killed *P. pentosaceus* TAP041 (MOI500). Data depict the mean ± SD of three independent experiments

cells treated with live LAB at MOI 250 displayed a significant capacity to induce IL-1β and COX-2 (334.9- and 704.9-fold, respectively) compared to the positive control. Heat-killed LAB at MOI 500 also induced IL-1β and COX-2, although lower than live LAB. IL-1β and COX-2 are known to be pro-inflammatory cytokines secreted by the inflammatory response. Thus, the mRNA expression levels of these cytokines indicate that *P. pentosaceus* TAP041 dosage significantly impacts the immunostimulatory effects, whether live or heat-killed. Considering cell cytotoxicity, heat-killed *P. pentosaceus* TAP041 may be deemed safe for further applications (Xu et al., 2023).

When RAW264.7 cells were treated with live and heat-killed *P. pentosaceus* TAP041, the protein expression levels of JNK, p38, and ERK were significantly increased (Fig. 5A-C). The JNK, p38, and ERK expression levels were markedly higher in LPS-induced macrophages than in untreated cells (40.4%, 35.0%, and 61.2%, respectively). Live *P. pentosaceus* TAP041 increased the levels of JNK, p38, and ERK phosphorylation in RAW264.7 cells compared to untreated cells. Moreover, there was no induction of phosphorylation of these proteins by heat-killed LAB relative to the untreated control group.

The MAPK signaling pathway is usually correlated with LPS-induced inflammation in immune cells and regulates various cellular responses. The MAPK signaling pathway, which includes JNK, p38, and ERK, mediates signaling responses in the immune and inflammatory systems. These results suggested that live and heat-killed *P. pentosaceus* TAP041 maintain a balance between M1/M2 macrophages by regulating pro-inflammatory and anti-inflammatory mediators (Shapouri-Moghaddam et al., 2018; Zhu et al., 2016).

Concludingly, *P. pentosaceus* TAP041 reduced the levels of GO and MGO in culture supernatants. The probiotic properties and immunostimulatory activities of this strain have been confirmed. This strain was demonstrated to be resistant to acid, bile salts, pancreatin, and lysozyme and to have higher gut adhesion and aggregation capacities. In the live and heat-killed state, the strain was confirmed to significantly enhance the expression levels of various cytokines such as iNOS, TNF-α, IL-6, IL-1β, and COX-2 and the expression levels of JNK, p38, and ERK protein in the MAPK signaling pathway. These findings suggest that both live and heat-killed *P. pentosaceus* TAP041 may act as immunostimulatory agents potentially applicable as a functional food additive and pharmacologically.

Supplementary Information The online version contains supplementary material available at https://doi.org/10.1007/s10068-024-01530-2.

Acknowledgements This study was supported by MetaCen Therapeutics.

Funding This work received support from MetaCen Therapeutics.

Declarations

Competing Interest The authors declare no conflict of interest.

References

Abdalla AK, Ayyash MM, Olaimat AN, Osaili TM, Al-Nabulsi AA, Shah NP, Holley R. Exopolysaccharides as antimicrobial agents: Mechanism and spectrum of activity. Frontiers in Microbiology 12: 664395 (2021)

Ayyash MM, Abdalla AK, AlKalbani NS, Baig MA, Turner MS, Liu SQ, Shah NP. Invited review: Characterization of new probiotics from dairy and nondairy products—Insights into acid tolerance, bile metabolism and tolerance, and adhesion capability. Journal of Dairy Science 104: 8363-8379 (2021)

Balgir PP, Kaur B, Kaur T, Daroch N, Kaur G. In vitro and in vivo survival and colonic adhesion of *Pediococcus acidilactici* MTCC5101 in human gut. BioMed Research International 2013: 583850 (2013)

Cao Z, Pan H, Tong H, Gu D, Li S, Xu Y, Ge C, Lin Q. In vitro evaluation of probiotic potential of *Pediococcus pentosaceus* L1 isolated from paocai—a Chinese fermented vegetable. Annals of Microbiology 66: 963-971 (2015)

Cho Y, Han HT, Kim TR, Sohn M, Park YS. Immunostimulatory activity of *Lactococcus lactis* LM1185 isolated from Hydrangea macrophylla. Food Science and Biotechnology 32: 497-506 (2023)

Coleman JW. Nitric oxide in immunity and inflammation. International immunopharmacology 1: 1397-1406 (2001)

du Toit M, Franz CMAP, Dicks LMT, Schillinger U, Haberer P, Warlies B, Ahrens F, Holzapfel WH. Characterisation and selection of probiotic lactobacilli for a preliminary minipig feeding trial and their effect on serum cholesterol levels, faeces pH and faeces moisture content. International Journal of Food Microbiology 40: 93-104 (1998)

FAO/WHO. Guidelinces for the evaluation of probiotics in food. FAO/WHO working group, 1–11 (2002)

Gaens KH, Stehouwer CD, Schalkwijk CG. Advanced glycation endproducts and its receptor for advanced glycation endproducts in obesity. Current Opinion in Lipidology 24: 4-11 (2013)

García-Ruiz A, González de Llano D, Esteban-Fernández A, Requena T, Bartolomé B, Moreno-Arribas MV. Assessment of probiotic properties in lactic acid bacteria isolated from wine. Food Microbiology. 44: 220-225 (2014)

Holt JG, Krieg NR, Sneath PH, Staley JT, Williams ST. Bergey's manual of determinative bacteriology. 9th. Baltimor: William & Wilkins (1994)

Jeong S, Kwon A, Jeong H, Park YS. Synergistic immunostimulatory activities of probiotic strains, *Leuconostoc lactis* and *Weissella cibaria*, and the prebiotic oligosaccharides they produce. Microorganisms 11: 1354 (2023)

Joung JA, You JY, Lee SS, Choi JH. Potential probiotic activity of isolated *Lactobacillus harbinensis* VF from taditionally fermented vinegar. Food Engineering Progress 27: 155-164 (2023)

Kwon HK, Song MJ, Lee HJ, Park TS, Kim MI, Park HJ, *Pediococcus pentosaceus*-fermented *Cordyceps militaris* inhibites inflammatory reactions and alleviates contact dermatitis. International Journal of Molecular Sciences. 9: 3504 (2018).

Lee KW, Park JY, Sa HD, Jeong JH, Jin DE, Heo HJ, Kim JH. Probiotic properties of *Pediococcus* strains isolated from jeotgals, salted and fermented Korean sea-food. Anaerobe 28: 199-206 (2014)

Lee MG, Joeng H, Shin J, Kim S, Lee C, Song Y, Lee BH, Park HG, Lee TH, Jiang HH, Han YS, Lee BG, Lee HJ, Park MJ, Jun YJ, Park YS. Potential probiotic properties of exopolysaccharide-producing *Lacticaseibacillus paracasei* EPS DA-BACS and prebiotic activity of its exopolysaccharide. Microorganisms 10: 2431 (2022)

Lin SW, Wu CH, Jao YC, Tsai YS, Chen YL, Chen CC, Fang TJ, Chau CF. Fermented supernatants of *Lactobacillus plantarum* GKM3 and *Bifidobacterium lactis* GKK2 protect against protein glycation and inhibit glycated protein ligation. Nutrients 15: 277 (2023)

Lin Y, Briandet R, Kovács ÁT. *Bacillus cereus* sensu lato biofilm formation and its ecological importance. Biofilm 4: 100070 (2022)

MacMicking J, Xie Qw, Nathan C. Nitric oxide and macrophage function. Annual review of immunology 15: 323-350 (1997)

Ocaña VS, Nader-Macías ME. Vaginal lactobacilli: self- and co-aggregating ability. British Journal of Biomedical Science 59: 183-190 (2002)

Ohn JE, Seol MK, Bae EY, Cho YJ, Jung HY, Kim BO. The potential probiotic and functional health effects of lactic acid bacteria isolated from traditional korean fermented foods. Journal of Life Science. 30: 581-591 (2020)

Park HY, Lee HB, Lee SY, Oh MJ, Ha SK, Do E, Lee HHL, Hur J, Lee KW, Nam MH, Park MG, Kim Y. *Lactococcus lactis* KF140 reduces dietary absorption of Nε - (carboxymethyl)lysine in rats and humans *via* β-galactosidase activity. Frontiers in Nutrition 9: 916262 (2022)

Pramanik S, Venkatraman S, Karthik P, Vaidyanathan VK. A systematic review on selection characterization and implementation of probiotics in human health. Food Science and Biotechnology 32: 423-440 (2023)

Sena CM, Matafome P, Crisóstomo J, Rodrigues L, Fernandes R, Pereira P, Seiça RM. Methylglyoxal promotes oxidative stress and endothelial dysfunction. Pharmacological Research 65: 497-506 (2012)

Shapouri-Moghaddam A, Mohammadian S, Vazini H, Taghadosi M, Esmaeili SA, Mardani F, Seifi B, Mohammadi A, Afshari JT, Sahebkar A. Macrophage plasticity, polarization, and function in health and disease. Journal of Cellular Physiology 233: 6425-6440 (2018)

Shin JS, Jung JY, Lee SG, Shin KS, Rhee YK, Lee MK, Hong HD, Lee KT. Exopolysaccharide fraction from *Pediococcus pentosaceus* KFT18 induces immunostimulatory activity in macrophages and immunosuppressed mice. Journal of Applied Microbiology 120: 1390-1402 (2016)

Shukla R, Goyal A. Probiotic potential of *Pediococcus pentosaceus* CRAG3: A new isolate from fermented cucumber. Probiotics and Antimicrobial Proteins 6: 11-21 (2014)

Suh KS, Choi EM, Rhee SY, Kim YS. Methylglyoxal induces oxidative stress and mitochondrial dysfunction in osteoblastic MC3T3-E1 cells. Free Radical Research 48: 206-17 (2014)

Tarique M, Abdalla A, Masad R, Al-Sbiei A, Kizhakkayil J, Osaili T, Olaimat A, Liu S-Q, Fernandez-Cabezudo M, al-Ramadi B, Ayyash M. Potential probiotics and postbiotic characteristics including immunomodulatory effects of lactic acid bacteria isolated from traditional yogurt-like products. Lwt 159: 113207 (2022)

Trunk T, Khalil HS, Leo JC. Bacterial autoaggregation. AIMS Microbiology 4: 140-164 (2018)

Uğur H, Görünmek M, Çatak J, Efe E, Özgür B, Duman S, Yaman M. Determination and assessment of the most potent precursors of advanced glycation end products in baklava and Turkish delight by HPLC. Food Science and Technology 42: e08522 (2022)

Xu X, Qiao Y, Peng Q, Shi B. Probiotic properties of *Loigolactobacillus coryniformis* NA-3 and in vitro comparative evaluation of live and heat-killed cells for antioxidant, anticancer and immunoregulatory activities. Foods 12: 1118 (2023)

Zhang H, Wang Z, Li Z, Wang K, Kong B, Chen Q. l-glycine and l-glutamic acid protect *Pediococcus pentosaceus* R1 against oxidative damage induced by hydrogen peroxide. Food Microbiology 101: 103897 (2022)

Zhu Y, Li X, Chen J, Chen T, Shi Z, Lei M, Zhang Y, Bai P, Li Y, Fei X. The pentacyclic triterpene Lupeol switches M1 macrophages to M2 and ameliorates experimental inflammatory bowel disease. International Immunopharmacology 30: 74-84 (2016)